RSC Advances

PAPER

View Article Online
View Journal | View Issue

Cite this: *RSC Adv.*, 2024, **14**, 14202

Preparation of imidazole-modified paper membrane for selective extraction of gallic acid and its structural and functional analogues from *Pomegranate Peel*†

Xiaoxue Sun,‡[a] Jingyu Zhang,‡[a] Xiaohui Han,[a] Shumin Li,[a] Xuerui Zhang[a] and Xiaodong Bi *[ab]

In the search for pharmaceutically active compounds from natural products, it is crucial and challenging to develop separation methods that target not only structurally similar compounds but also a class of compounds with desired pharmaceutical functions. To achieve both structure-oriented and function-oriented selectivity, the choice of functional monomers with broad interactions or even biomimetic roles towards targeted compounds is essential. In this work, an imidazole (IM)-functionalized paper membrane was synthesized to realize selectivity. The IM was selected based on its capability to provide multiple interactions, participation in several bioprocesses, and experimental verification of adsorption performance. Using gallic acid as a representative component of *Pomegranate Peel*, the preparation conditions and extraction parameters were systematically investigated. The optimal membrane solid-phase extraction (MSPE) method allowed for enrichment of gallic acid from the complex matrix of *Pomegranate Peel*, enabling facile quantitative analysis with a limit of detection (LOD) of 0.1 ng mL^{-1}. Furthermore, with the aid of cheminformatics, the extracted compounds were found to be similar in both their structures and pharmaceutical functions. This work offers a novel approach to preparing a readily synthesized extraction membrane capable of isolating compounds with similar structures and pharmaceutical effects, and provides an MSPE-based analytical method for natural products.

Received 15th December 2023
Accepted 17th April 2024

DOI: 10.1039/d3ra08576g

rsc.li/rsc-advances

1. Introduction

Natural products, including herbs and microorganisms, are one of the most important sources for drug discovery.[1–3] Besides screening for active compounds, how to separate these targets from their complex matrix is a key technical issue.[4–6] Membrane technology,[7] due to its selective permeation or retention and diverse application forms, has been widely used in the processes of separation, concentration, or purification of natural products with various industrial and scientific purposes.[8,9] As for regulating membrane affinity, which is a research focus and challenge, concept and practice have gradually evolved from extracting compounds with specific structures (structure-oriented) to extracting a class of compounds with desired pharmaceutical functions (function-oriented). There are several methods that could be referenced: (1) extrathermodynamics-based research: the relationship between chromatographic retention and physicochemical parameters of tested compounds has been described by means of linear free energy relationships (LFERs) or other derivative methods,[10–12] for better summarizing an applicable range of tested adsorbents and predicting separation conditions for new targets. (2) Biomimetic methods: the target molecule[13–15] (such as protein) or tissue[16–18] (such as a cytomembrane) for a drug is introduced in the *in vitro* separation medium as a functional monomer, producing a target-specific interaction, which links the retention behavior directly to biological function. (3) Big data methods:[19–22] the experimental data are collected from current research literature and analyzed by artificial intelligence algorithms either to help design or choose adsorbents or to establish the relationship between the structures of the extracted compounds and their pharmaceutical functions. Moreover, the design of functional membranes for natural products should not interfere with their pharmaceutical activities and should be convenient for scale-up experiments. Considering the complexity of natural products, it is still a challenge to design a specific functional membrane to extract desired compounds with similar structures or functions from one natural origin.

[a]*School of Pharmaceutical Sciences & Institute of Materia Medica, Shandong First Medical University & Shandong Academy of Medical Sciences, Jinan 250117, Shandong, China. E-mail: xiaodongb_pharm@126.com*

[b]*Key Laboratory for Biotechnology Drugs of National Health Commission (Shandong Academy of Medical Sciences), Jinan 250117, Shandong, China*

† Electronic supplementary information (ESI) available: Appendix A: supplementary data. See DOI: https://doi.org/10.1039/d3ra08576g

‡ X. Sun and J. Zhang contributed equally.

The imidazole (IM) ring, due to its widespread presence in the structures of many natural and metabolically active substances (such as histidine) and its involvement in corresponding biological processes,[23] can provide abundant interactions (such as hydrogen bonding or π–π interaction)[24] with numerous bioactive compounds. Hence it has been utilized as an important bio-isostere for synthesizing new drugs in medicinal chemistry[25,26] and even as a functional building block in materials science.[27] For integration with functional membranes, several forms have been developed through outstanding approaches in materials science, such as the derivatives of IM,[28] IM-based ionic liquids,[29] polymers containing IM,[30] and IM-type metal–organic frameworks (MOFs).[31] To regulate selectivity, IM as a functional monomer, alone or combined with other chemical groups, can be used for the adsorption or sensing of antibiotics,[32,33] pesticides,[33] salicylic acid,[34] or metal ions.[35] For further enhancement, the application of molecularly imprinted polymers (MIPs),[36–40] especially using IM-type functional monomers and template-induced cavities,[41] can achieve tailor-made selectivity towards a target compound or a class of compounds. Due to the rich interactions of imidazole and its potential in the regulation of selectivity, membrane materials developed based on imidazole are expected to target a class of compounds with similar structures. And, according to the principle that structurally similar compounds have analogous functions, this structure-oriented extraction can be converted to function-oriented extraction after further exploration of whether these extracted compounds share common biological functions.

In this work, an imidazole (IM)-modified paper membrane was synthesized *via* a microwave-accelerated polymerization reaction and utilized for membrane solid-phase extraction (MSPE). The porous fiber filter paper[42] (called a paper membrane) was selected as the support material for its easy modification and facile integration into the extraction process. Gallic acid (GA), one of the phenolic acid type components in *Pomegranate Peel*[43] and also the characteristic component of *Pomegranate Peel* prescribed by Chinese pharmacopeia,[44] was chosen as the test sample. In previous research, adsorbents for GA were C-18,[45] Ni–Co layered double hydroxides (LDH)[46] or MIPs.[47–51] Among these MIPs, 4-vinylpyridine[50] or dopamine[51] was used as functional monomer, indicating that nitrogen-containing structures could interact with GA. However, functional monomers and template-induced cavities worked together in MIPs, which required skilled synthesis. Therefore, we attempted to use a facile preparation method. Theoretically, the basis for interaction between IM (a nitrogen-containing five-membered heterocyclic ring) and GA (a phenolic acid structure) is through hydrogen bonding and π–π interaction.[24] Methylacrylic acid (with –OH to provide hydrogen bonding instead of nitrogen) and butyl methacrylate (with hydrophobic attraction *via* the carbon chain) were first selected for comparison with IM. After validating the function of IM, GA was used to investigate the preparation conditions, operational parameters, and quantitative capabilities of the IM-functionalized membrane. Qualitative analysis was performed by mass spectrometry (MS) to identify the compounds extracted from *Pomegranate Peel* using the MSPE method. Subsequently, cheminformatics analysis was conducted to assess whether the identified compounds shared common structural features and biological activities (for the scheme, see Fig. 1). This research offered a novel approach for preparing a readily synthesized extraction membrane capable of extracting compounds with similar structures and pharmaceutical effects, as well as an MSPE-based analytical method for natural products.

2. Materials and methods

2.1. Reagents and materials

1-Allyl-1*H*-imidazole (1-IM), butyl methacrylate (BMA), ethylene glycol dimethacrylate (EGDMA, stabilized with HQ), 2,2′-azobis(isobutyronitrile) (AIBN), and γ-methacryloxypropyltrimethoxysilane (γ-MAPS) were purchased from Tokyo Chemical Industry (TCI-Shanghai, China). Polyhedral oligomeric silsesquioxane (POSS, methacryl substituted. Cage mixture, $n = 8$, 10, 12) was purchased from Sigma-Aldrich (Shanghai, China). Methylacrylic acid (MA) was purchased from Shanghai Maclin Biochemical Technology Co., Ltd. Dimethyl sulfoxide (DMSO), methanol (HPLC grade), acetonitrile (HPLC grade), acetic acid (HAc), ammonium hydroxide, NaOH, gallic acid (GA), powder of *Pomegranate Peel*, and PTFE porous membranes (0.22 μm) were purchased from Jinan Reagent Company. Whatman paper membranes (circular, diameter = 25 mm) were obtained from GE Healthcare UK Ltd. A chromatographic Agilent ZORBAX Eclipse Plus C18 (3 × 100 mm, 1.8 μm) column and Waters BEH C8 column (100 mm × 2.1 mm, 1.7 μm) (Waters, Milford, MA) were used for LC and LC-TOF/MS, respectively. Pure water (Wahaha Co. Ltd, China) was used for the mobile phase and all other experiments.

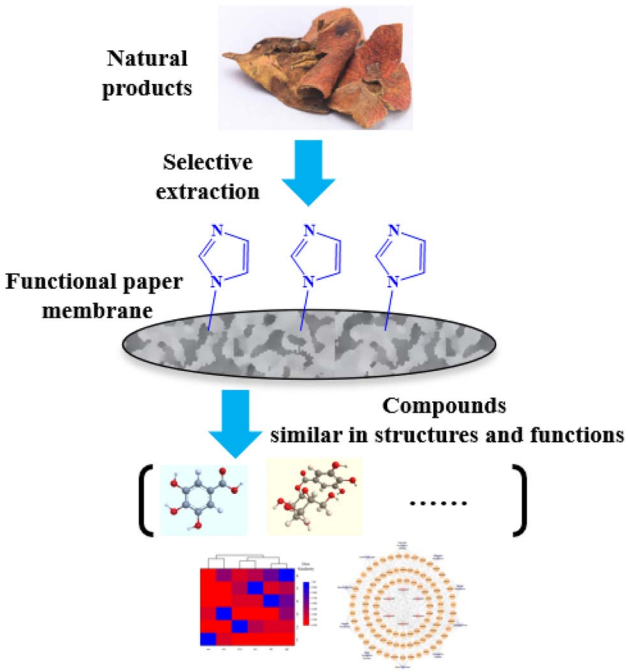

Fig. 1 Scheme of this work. An IM-functionalized paper membrane could extract compounds with structural and functional similarities.

2.2. Instruments

An Ultimate 3000 UHPLC System (Thermo, USA) was used for liquid chromatography experiments. LC-TOF/MS was performed on a UPLC (Waters, Milford, MA)-Q Exactive HF MS (Thermo Fisher Scientific, Rockford, IL, USA). A Midea microwave oven (max power = 1000 W, Guangdong, China) was used for synthesizing extraction membranes. A Saipurui SPE device with 24 ports (Tianjin, China) was used to perform membrane extraction. An Anyan nitrogen blow-drying apparatus (Hangzhou, China) was used for concentration. A Waters UPLC-Q Exactive HF MS System (Thermo Fisher Scientific, Rockford, IL, USA) was used for identification. IR and SEM characterization were performed on a Spectrum 100 FT-IR spectrometer (PerkinElmer Inc., Waltham, Massachusetts, USA) equipped with a DTGS detector, and Zeiss Ultra-55 field emission scanning electron microscopy.

2.3. Preparation of the extraction membrane and investigation of preparation conditions

The preparation procedures were adapted from our previous work.[52] Three main steps were involved: (1) pretreatment of the filter membranes: the original membranes were soaked in a 1 mol L^{-1} NaOH aqueous solution for 12 hours at room temperature (RT), then rinsed with water until the pH was neutral (pH = 7). Methanol was used to remove residual water, and the membranes were dried at 60 °C. (2) Modification with C=C groups: the pretreated membranes were soaked in a 40% solution of γ-MAPS methanol for 24 hours at RT. After this time, they were washed with methanol to remove excess γ-MAPS and subsequently dried at 60 °C. (3) Preparation of 1-IM modified membranes (extraction membranes): a reaction mixture was prepared by dissolving a monomer, crosslinker, and 5 mg of AIBN in 300 μL of DMSO (the specific composition is detailed in subsequent investigations). The mixture was added dropwise onto the triple layers of C=C modified membranes to ensure full absorption. The membranes were then placed in a microwave oven and heated at 1000 W for 15 minutes. Once the reaction was complete, the extraction membranes were cleaned with methanol to remove any unreacted materials and dried at 60 °C. The finalized extraction membranes were sealed and stored at RT for future use.

For the extraction tests, the extraction membranes were assembled into a solid phase extraction (SPE) device as follows: three layers of extraction membranes were sandwiched between two PTFE membranes, forming a membrane group that was secured within a needle filter. The upper part of the needle filter was connected to a 5 mL syringe, and the lower end was fixed to an SPE vacuum pump interface *via* a flow-limiting valve.

The univariate method was employed to investigate preparation conditions, altering one variable at a time. The optimal factor identified was then used in subsequent experiments. The detailed investigation included: (1) examining three types of monomer (containing a carboxyl group, an alkyl chain, or imidazole, namely MA, BMA, or 1-IM), using 5 μL of 1-IM and 25 μL of EDGMA; for MA or BMA, their amounts were equimolar to 1-IM. (2) Varying the quantity of the selected monomer (5 μL, 10 μL, 20 μL, or 50 μL). (3) Adding either 5 μL or 10 μL of POSS as an additional crosslinker to assess whether mixed crosslinkers enhanced the immobilization of the monomer. To confirm the origin of the extraction functionality, three layers of pristine membranes (pure paper) and three layers of EDGMA-modified membranes were tested in the SPE device.

2.4. Extraction tests

Before each extraction, the membranes were pre-cleaned and checked for leakage using 5 mL of methanol followed by 5 mL of acetonitrile. During the extraction tests, samples were passed through the membrane and collected into a tube within the SPE device chamber.

For investigation of the preparation conditions, the test sample was a 20 μg mL^{-1} GA solution prepared by diluting a 2 mg mL^{-1} GA stock solution (dissolved in methanol) with water. The adsorption ratio was calculated as the ratio of the chromatographic peak area of the initial sample to that of the filtered sample. To facilitate comparison between different preparation conditions, the sample was filtered and collected only once. Chromatographic conditions for the extraction tests included a mobile phase composed of acetonitrile (A) and water with 0.1% acetic acid (B) at a ratio of 5 : 95. The injection volume was set to 20 μL, with a flow rate of 0.3 mL min^{-1}. The temperature of the column compartment was maintained at 30 °C, and absorbance was measured at 270 nm. Results were collected from three groups of membranes prepared under the same conditions.

Optimization of SPE parameters involved various samples and extraction tests: (1) to investigate the effect of sample solvent, GA stock solutions were diluted with water, methanol, or acetonitrile to prepare 20 μg mL^{-1} GA solutions. Samples diluted in methanol or acetonitrile were further diluted 1 : 1 (v/v) with water before LC analysis. The injection volume was adjusted to 4 μL due to lower column efficiency being observed with larger volumes or without water dilution. (2) To study the pH effect, water was used as the diluent with the addition of 1% acetic acid. (3) For investigation of extraction times, the same 20 μg mL^{-1} GA aqueous solution was filtered through the same membrane multiple times consecutively. (4) Elution solutions were tested using the optimal extraction time; solutions included methanol and mixtures of acetonitrile and methanol, all containing 0.1% acetic acid. (5) Elution times were investigated using the optimal extraction time and eluent, eluting the membrane multiple times in succession. In studies involving elution solutions and times, samples were diluted 1 : 1 (v/v) with water and injected at 4 μL for LC analysis. Results were collected from three groups of membranes prepared under the same conditions for each part of this optimization process.

2.5. Preparation of the *Pomegranate Peel* extract

0.1 g of *Pomegranate Peel* powder was thoroughly dispersed in 2.0 mL of a 75% (v/v) methanol aqueous solution. The mixture was then sonicated for 20 minutes and subsequently filtered to obtain the supernatant. For MSPE testing, the prepared supernatant was diluted 10-fold with water (the dilution solvent was chosen based on the results of the solvent effect study) to yield

the extract. Dilution was necessary to prevent an overload LC signal due to the MSPE-processed sample (data not shown). For LC-TOF/MS analysis, the supernatant was used without dilution. Prior to use, the extract was stored at 4 °C and utilized within the same day.

2.6. Quantitative and qualitative performance of MSPE

To build the standard curve, a series of concentrations (0.5 ng mL^{-1}, 1 ng mL^{-1}, 2 ng mL^{-1}, 5 ng mL^{-1}, 10 ng mL^{-1}, 20 ng mL^{-1}, 50 ng mL^{-1}, 100 ng mL^{-1}, 200 ng mL^{-1}, 500 ng mL^{-1}) of GA aqueous solution were prepared. The elutes were collected under the optimal MSPE conditions, and blown dry under nitrogen, and then dissolved again by 250 μL of 5% (v/v) methanol aqueous solution for each one. These re-dissolved solutions were analyzed by LC to collect the peak areas. LC conditions included a mobile phase composed of (A) acetonitrile and (B) 0.1% aqueous acetic acid (HAc), with a gradient from 100% to 92% B over 0–5 min, 92% to 75% B over 5.1–15 min, 20% B at 15.1–20 min, and back to 100% B over 20.1–25 min. The injection volume was set to 10 μL, with a flow rate of 0.3 mL min^{-1}. The temperature of the column compartment was maintained at 30 °C, and absorbance was measured at 270 nm. For each concentration level, three samples were tested on one membrane group to ensure consistent results.

Additionally, the eluate was collected for identification of captured compounds by LC-TOF/MS. The LC-TOF/MS conditions were as follows: for the LC part, the temperature of the column compartment was set to 50 °C, the flow rate to 0.3 mL min^{-1}, and the injection volume to 2 μL. The mobile phase consisted of (A) 0.1% aqueous HAc and (B) acetonitrile, with a gradient from 8% to 80% B over 5–15 min, then to 100% B over 15–15.5 min, holding until 18 min before returning to 8% B over 18–18.5 min, and maintaining until 22 min. For the MS part, the full scan range was *m*/*z* 70–1050, with a spray voltage of 3.50 kV for positive ionization and 3 kV for negative ionization. The capillary temperature was set to 300 °C, with the sheath gas temperature at 350 °C. Sheath gas and auxiliary gas flow rates were set to 45 and 10 (arbitrary units), respectively. The resolution was set to $12e^4$, with the resolution of dd-MS^2 at $3e^4$. The top 10 compounds were selected for secondary data acquisition, with a collision energy NCE of 30. For qualitative analysis, the molecular weight and tandem mass spectrometry (MS/MS) data were matched against an MS database that was compiled using standard reference substances.

Finally, cheminformatics tools were applied to analyze structural similarities or biological effects among these compounds. The structural similarity was calculated by a molecular fingerprint-based method. The results were presented as the Dice index.[53] The functional similarity was estimated by network pharmacology (by using the Swiss Target Prediction database[54]).

3. Results and discussion

3.1. Investigation of preparation conditions

IM can have many interactions with other molecules.[24] Specifically, for interactions between IM and GA, there are two major parts: (1) a phenolic hydroxyl group and a carboxyl group can interact with nitrogen on the imidazole ring *via* hydrogen bonding, (2) while benzene in phenolic acid can provide π–π interaction when close to and parallel with the imidazole ring. For comparison, oxygen-containing methylacrylic acid was chosen to contrast with nitrogen-containing imidazole in terms of hydrogen bonding strength. Meanwhile, butyl methacrylate, which features a carbon chain, was used in place of a ring structure to provide hydrophobic attraction. For experimental verification, these three different types of monomers showed different performances (see Fig. 2A). The test sample was an aqueous solution of GA (20 μg mL^{-1}) with a pH of around 5.5, which was higher than the pK_{a1} of GA (around 4.4) or pK_a of a carboxyl group in MA (around 4.2). As a result, both GA and MA were negatively charged and mutually exclusive in the aqueous solution. This explained why the MA monomer showed poor adsorption towards GA. In this part, MA and other monomers were not further compared in the acid-added sample, because additional pH adjustment would require supplementary additives, which might interfere with the activity of the components and complicate the extraction process. Regarding BMA, this non-charged monomer, the adsorption ratio was improved (2.3 times higher than that of MA) due to the hydrophobic force of its alkyl chain. The pK_a of the IM ring was around 6.9, which was partly ionized in the test sample solution and contributed to adsorption *via* electrostatic attraction, thus showing the best performance (the adsorption ratio was around 0.66). Next, the amount of 1-IM was explored (see Fig. 2B). When the amount of 1-IM increased from 5 μL to 20 μL, the adsorption ratio became 1.3 times higher. However, when it reached 50 μL, the adsorption ratio decreased, possibly due to the excessive amount of monomer leading to higher crosslinking density and a decrease in the number of interactive sites. Therefore, the amount of 1-IM was set at 20 μL for the remaining experiments. To confirm the function of the 1-IM monomer, comparisons were made among 1-IM modified membrane, EDGMA modified membrane (without 1-IM), and pure paper membrane (without 1-IM or crosslinker) (see Fig. 2C). The results demonstrated that both 1-IM monomer and EDGMA (with a similar structure to BMA) contributed to the adsorption through hydrogen bonding, π–π stacking, and hydrophobic interaction of the alkyl chain, with the adsorption ratio of 1-IM being 1.3 times higher (the adsorption ratio was around 0.86) than that of EGDMA alone. Finally, a second crosslinker, POSS,[55,56] which was proven to enhance separation, was added to check whether the monomer was well distributed and immobilized on the paper membrane (see Fig. 2D). When POSS started to participate (from 0 to 5 mg), the adsorption ratio decreased by nearly 23% due to its occupation of reactive sites for the 1-IM monomer. However, when the amount reached 10 mg, the adsorption ratio rose over 90%, indicating that POSS began to enhance adsorption due to its cage-like structure for a higher density of immobilized monomers. Nevertheless, the adsorption ratio did not improve sharply and considering the price of POSS (higher than EDGMA), no further use of POSS was pursued. In summary, the optimal reactants were 20 μL of 1-IM, 25 μL of EDGMA, and 5 mg of AIBN in 300 μL of DMSO.

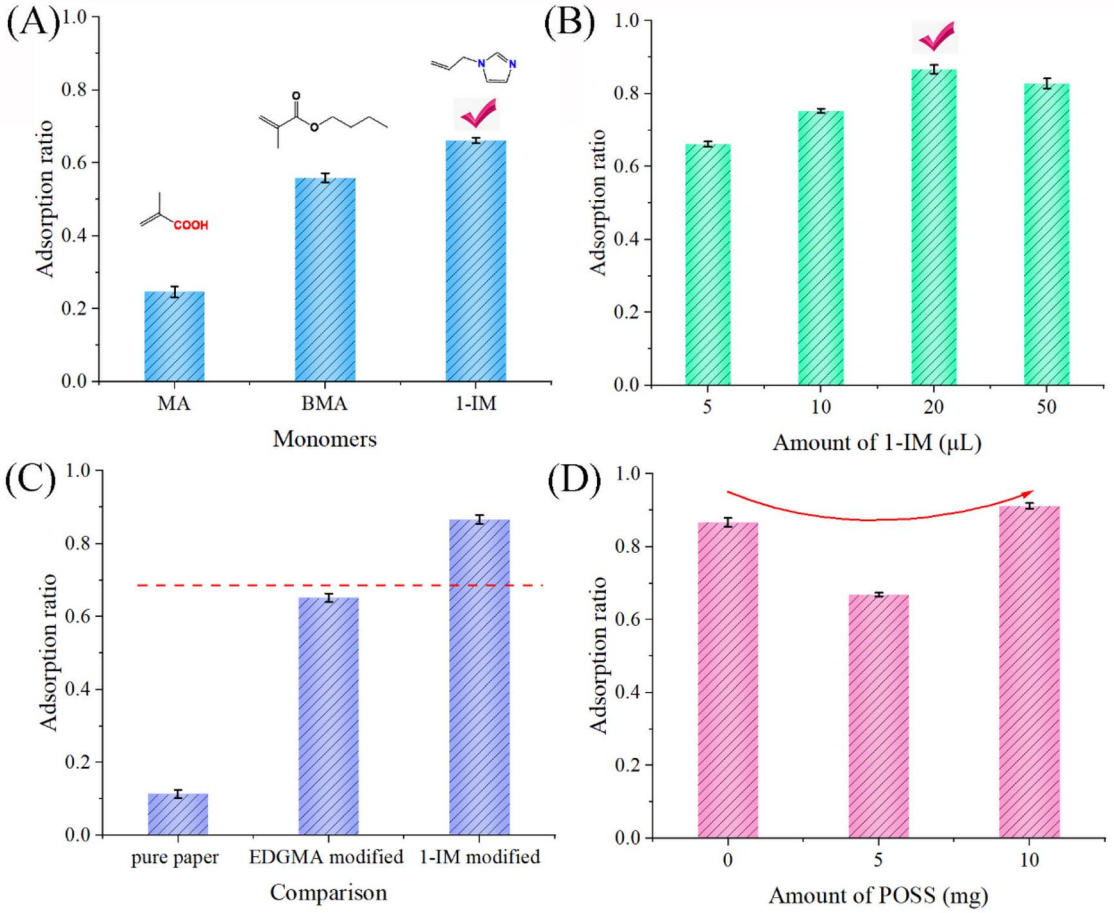

Fig. 2 Investigation of preparation conditions: (A) comparison of monomers, (B) amount of 1-IM, (C) comparison with other controls, and (D) amount of POSS.

3.2. Characterization of the membrane

ATR-IR and SEM were used to characterize the membrane materials (see Fig. 3). The IR data (see Fig. 3A) were normalized by reflectivity, ranging from 0 to 100 for qualitative analysis. After C=C modification, a peak at 1718.23 cm^{-1} was observed, indicating successful modification of C=C. After reaction with 1-IM, the peak at 1718.23 cm^{-1} decreased, while a weak peak at 1720.30 cm^{-1} remained, suggesting that C=C was consumed during the reaction and that EDGMA (containing C=O) and imidazole (containing C=C and C=N) were immobilized. According to the IR database (Spectral Database for Organic Compounds, SDBS),[57] the 1-methylimidazole structure exhibits signals at 2916 cm^{-1}, 1473 cm^{-1}, 1285 cm^{-1}, and 1028 cm^{-1}. The peaks were consistent in those from 1-IM@paper. SEM analysis (see Fig. 3B–D) revealed different morphologies, which also reflected different modification steps. Due to the interference of the background from the paper itself, the energy spectrum is not shown.

3.3. Optimization of influential factors for MSPE

Influential factors were investigated using a univariate approach. First, the effect of diluting solvents (water, methanol, and acetonitrile) on the test sample was compared (Fig. 4A). The 1-IM modified membrane showed much better performance in water than in methanol or acetonitrile. A possible reason is that in organic solvents both GA and IM were not ionized, leading to weaker interaction than in water. Since GA is unstable (easily oxidized) in alkaline solution, only water and 1% HCOOH aqueous solution of GA were compared. With acid added, GA remained primarily in molecular form and IM became protonated, reducing adsorption (Fig. 4B). Based on the initial findings, methanol, acetonitrile, and HCOOH were considered as candidates for the elution solvent. When a sample was filtered multiple times using the same membrane (referred to as extraction times; see Fig. 4C), the adsorption ratio increased and began to plateau after three repetitions (around 0.97). The optimal elution solvent was found to be a mixture of methanol and acetonitrile (8 : 2) containing 1% HCOOH (see Fig. 4D). Nearly 96% of the adsorbed GA could be eluted in a single step. Consequently, these optimized MSPE parameters were used in subsequent experiments.

3.4. Binding isotherms and breakthrough parameters

The binding isotherms (see Fig. 5A) of MSPE for GA samples were obtained under the optimal parameters. The ratio of signal to noise (S/N) at 0.5 ng mL^{-1} was 12.4 (calculated by peak

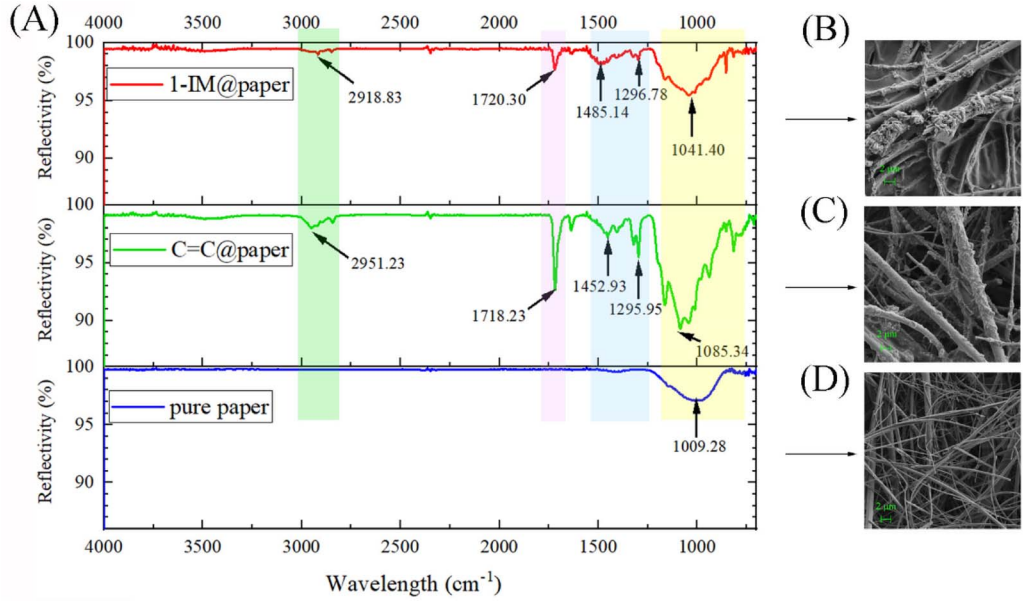

Fig. 3 Characterization: (A) ATR-IR. SEM (magnification: 10 K) for (B) 1-IM@paper, (C) C=C@paper, and (D) pure paper.

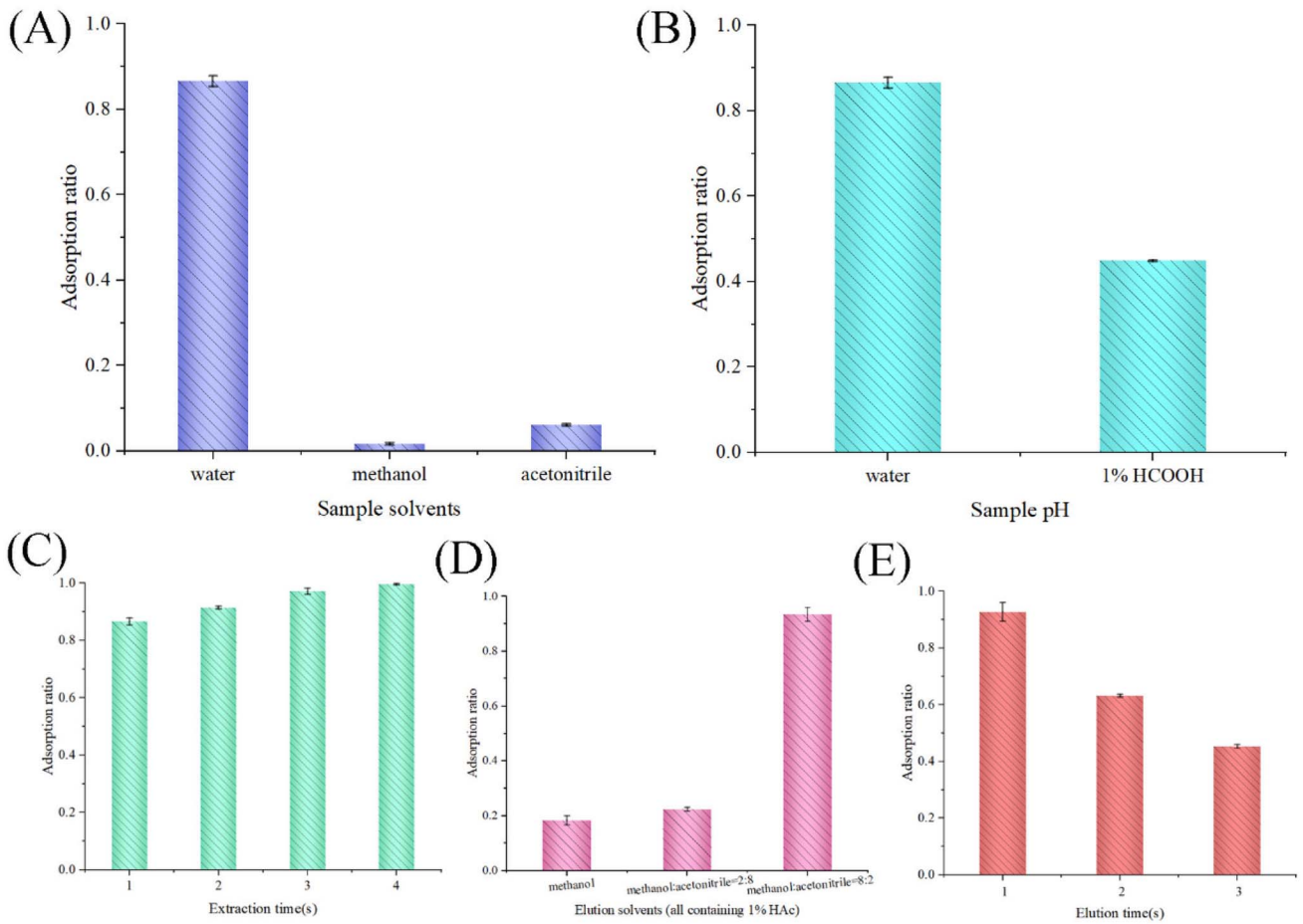

Fig. 4 Investigation of influential factors: (A) sample solvents, (B) sample pH, (C) extraction times, (D) elution solutions, and (E) elution times.

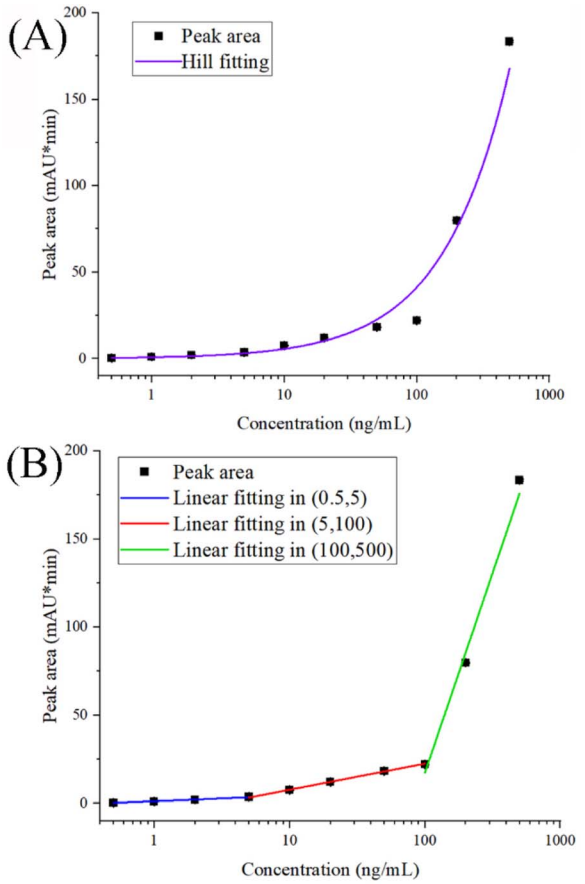

Fig. 5 Data fitting: (A) Hill fitting and (B) linear fitting.

height). According to the requirements of S/N for the limit of detection (LOD, S/N ≥ 3) and limit of quantitation (LOQ, S/N ≥ 10), the calculated LOD and LOQ were 0.1 ng mL^{-1} and 0.4 ng mL^{-1}, respectively. Both LOD and LOQ were much lower than those of HPLC (usually around 500–1000 ng mL^{-1}) and were even comparable to those of an MS detector. The binding isotherm was obtained by converting the *X*-axis coordinates to a base-10 scale and applying the Hill equation[58] (eqn (1), shown below).

$$y = B_{max}x^n/(x^n + K_d{}^n) \quad (1)$$

where B_{max} is the maximum binding, K_d is the dissociation constant, and n is the Hill slope; when $n < 1$, it indicates negatively cooperative binding. The fitting results, obtained by iterative computation, were: $B_{max} = 1.26$ mg mL^{-1}, $n = 0.87$, and $K_d = 14.36$ mg mL^{-1} ($R^2 = 0.95$). The order of magnitude of K_d (in mg mL^{-1}) suggests that the interaction was not strong, at least not comparable to that of IM-based molecularly imprinted materials. This could help maintain the activity of the eluted compounds and provide a basis for purification. The B_{max} was a theoretical fitting result, and for concentrations over 500 ng mL^{-1}, an earlier plateau or inflection point might appear before B_{max}. Since concentrations above 500 ng mL^{-1} can be directly analyzed by the LC-UV method, there is no need for MSPE enrichment and the upper concentration was set at 500 ng mL^{-1}. Due to nonlinearity throughout the entire range, linear fitting was performed in three separate ranges (see Fig. 5B): (1) for 0.5 ng mL^{-1} to 5 ng mL^{-1}, $R^2 = 0.994$, (2) for 5 ng mL^{-1} to 100 ng mL^{-1}, $R^2 = 0.998$, and (3) for 100 ng mL^{-1} to 500 ng mL^{-1}, $R^2 = 0.988$. This phenomenon of nonlinearity was also observed in previous research, particularly in flow-based extraction processes. This may be due to flow-induced molecular diffusion or other complex process factors.

The breakthrough curve is an important dynamic feature for a membrane filter process. Because (1) the sample volume is 5 mL, and (2) interval sampling is difficult over the whole filtering process, we apply simulation by computational fluid mechanics (CFD) to obtain the breakthrough curve (for detailed information about the CFD simulation, see Table S2†). CFD simulation is widely used in engineering and process control.[52] The results were: the adsorption rate constant is 0.052 s^{-1}, the breakthrough time is 96.5 s, and the breakthrough amount (at 96.5 s) is 0.057 mg (Fig. 6).

3.5. Application in quantitative and qualitative analysis of pomegranate peel

The quantitative capability of the MSPE was assessed using GA. The GA amount extracted from pomegranate peel power was (1.84 ± 0.054) μg g^{-1} (by fitting in the range of 5–100 ng mL^{-1}, for the LC profile of the MSPE; see Fig. 7). The run-to-run relative standard deviation (RSD) was 2.98%, calculated based on peak area. The batch-to-batch RSD was 13.4%, also calculated based on peak area. The recovery was 82.1–92.9% (at 500 ng mL^{-1}). For a comparison of methods, see Table S1.†

High-resolution LC-TOF/MS was used for qualitative analysis of the extracted compounds. For better identification, the undiluted extract of pomegranate peel powder was used directly as the MSPE sample (5 mL per sample). The eluted solution (5 mL) from MPME was then concentrated to 250 μL and submitted for direct LC-TOF/MS analysis. Since no other identification methods such as NMR were applied, we set a filter of

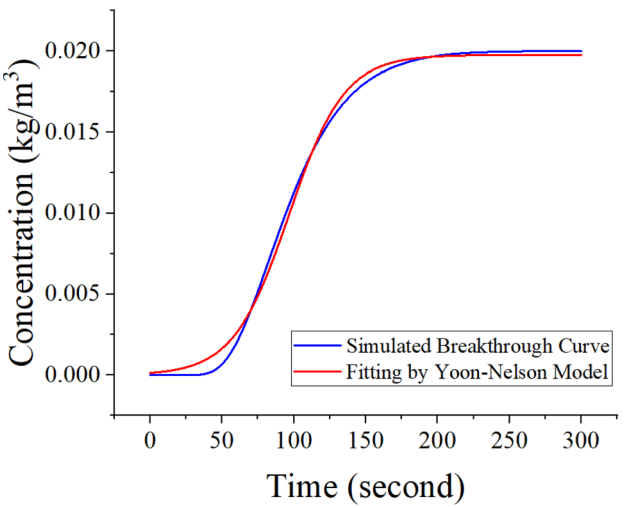

Fig. 6 CFD simulation of breakthrough curve and fitting by the Yoon–Nelson model (the R^2 of fitting by the Yoon–Nelson Model is 0.997).

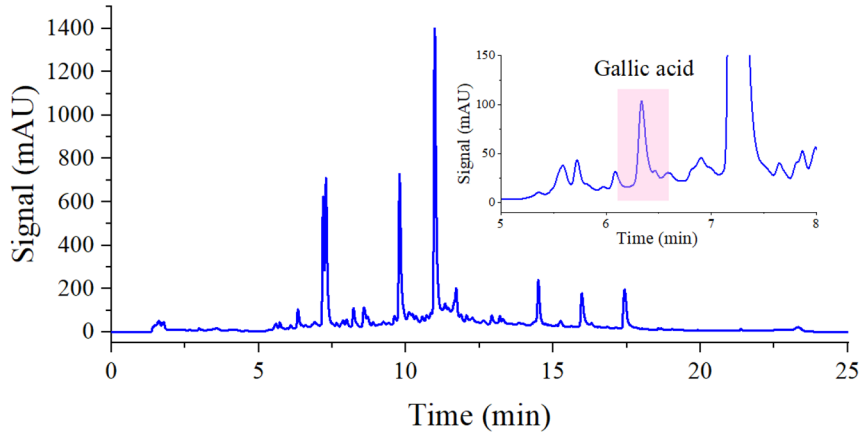

Fig. 7 Chromatogram of MPSE-proposed *Pomegranate Peel* extract.

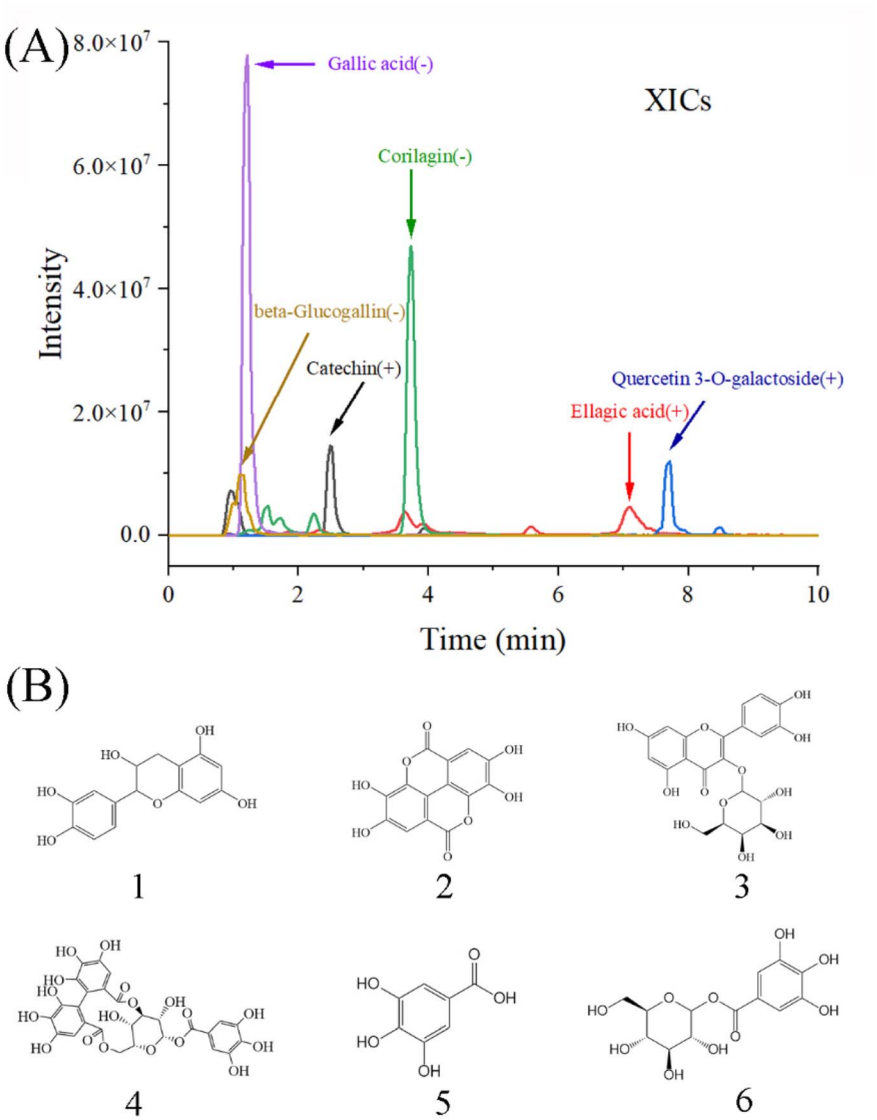

Fig. 8 XICs (A) and structure (B) for compounds **1–6**: **1** – catechin, **2** – ellagic acid, **3** – quercetin 3-*O*-galactoside, **4** – corilagin, **5** – gallic acid, and **6** – beta-glucogallin.

"peak area exceeding 1.0×10^8" to filter out relatively weak signals. Therefore, only six compounds were left for further analysis from the preliminary matching results including dozens of compounds (for MS information, see Table S2†) The XICs (extraction ion chromatograms) and corresponding structures are displayed in Fig. 8. For TICs (total ion

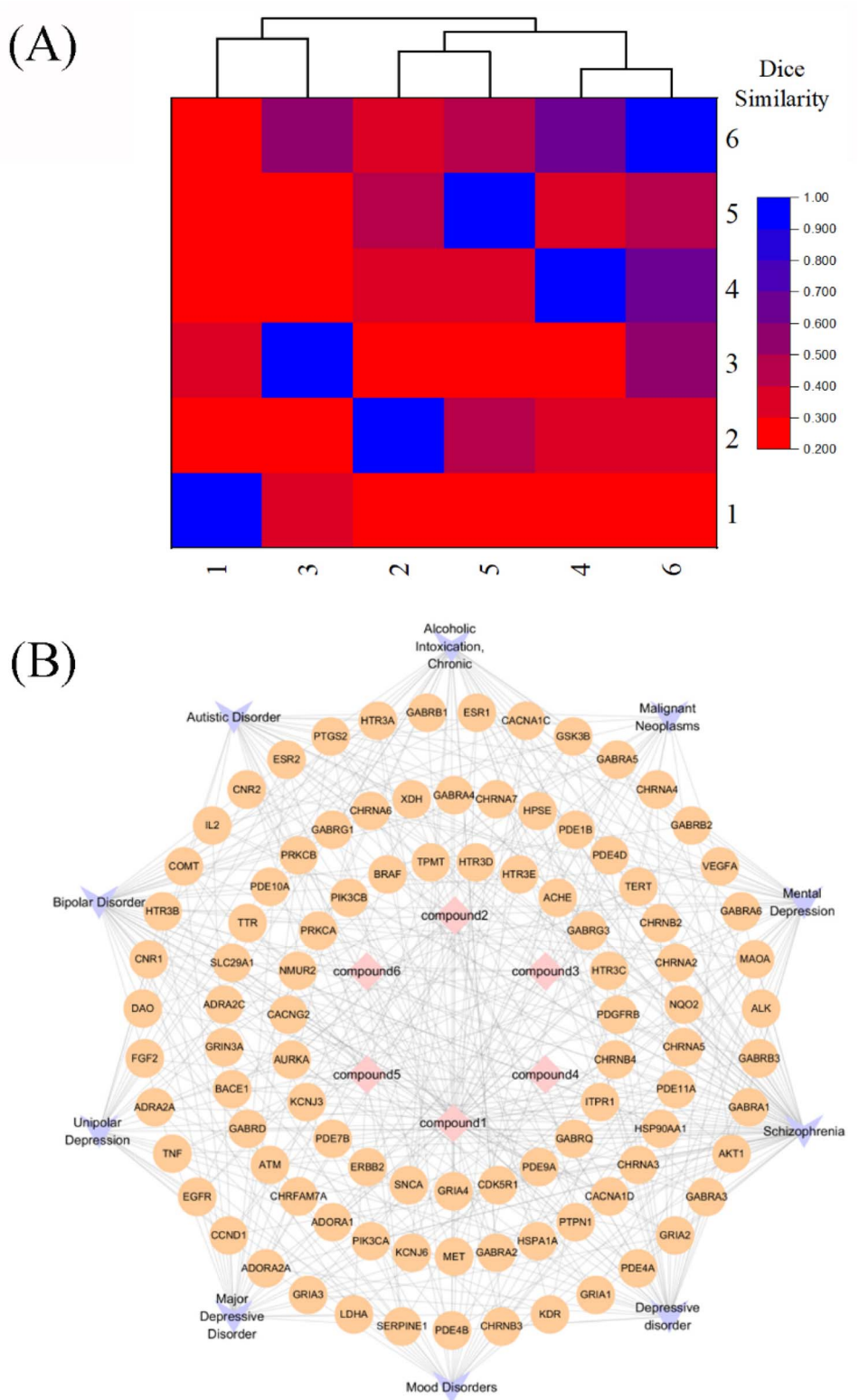

Fig. 9 Cheminformatic analysis: (A) structural similarity (by dice index, the numbers on the *x*-axis and *y*-axis represent compound number); (B) functional similarity (by network pharmacology, red represents compound number, yellow represents gene target, purple represents disease, detailed information of gene target referenced to the Swiss Target Prediction database).

chromatography) of ESI (±), primary MS and secondary MS for each compound, see Fig. S1–S8.† From the structures, the extracted compounds all had phenolic hydroxyl groups. Using a molecular-fingerprint-based method, the structural similarity, quantified using the Dice index[53] (Fig. 9A), was analyzed by hierarchical cluster analysis (HCA). Compounds **2** and **5**, **4** and **6**, **1** and **3**, were like each other at the first hierarchical level. Two groups, compounds **2** and **5**, and compounds **4** and **6**, were clustered together at the second hierarchical level. Correlation analysis and HCA provided a clearer description of the structural similarities. Network pharmacology, using the Swiss Target Prediction database,[54] was also employed to investigate functional similarities (see Fig. 9B), including gene targets and associated diseases. There were common gene targets among these extracted compounds, and their pharmaceutical effects were focused on ten diseases. Based on the results of chemoinformatics, there were similarities in both the structures and pharmaceutical functions of the extracted compounds. Hence, components that can interact with imidazole share common or similar structures. Following the principle that structurally similar compounds have analogous functions, these compounds with similar structures exhibit comparable pharmacological activities. This is the plausible molecular mechanism of function-oriented selectivity. Apart from experimental approaches,[59,60] the adsorbents can estimate the function[61] more than daily analysis.

4. Conclusions

In this work, an imidazole (IM)-functionalized paper membrane was synthesized for both structure-oriented and function-oriented selective extraction from the natural product pomegranate peel. IM was selected based on its capability to provide multiple interactions, participation in several bioprocesses, and experimental verification of adsorption performance. The preparation conditions and extraction parameters were systematically investigated using gallic acid as the representative component. The refined membrane solid-phase extraction (MSPE) method can be used to enrich gallic acid from the complex matrix of pomegranate peel, achieving a limit of detection (LOD) of 0.2 ng mL^{-1}. Extracted compounds were qualitatively identified by LC-TOF/MS and found to share structural and functional similarities, as determined by chem-informatics analysis. This work offers a novel approach for preparing a readily synthesized extraction membrane capable of extracting compounds with similar structures and pharmaceutical effects, along with an MSPE-based analytical method for natural products. Moreover, this design of selective affinity can be adapted for large-scale purification, aimed at the rapid discovery of pharmaceutically active compounds in natural products, especially those that are structural derivatives or functional analogues of a prodrug molecule.

Author contributions

Xiaoxue Sun and Jingyu Zhang: methodology, data curation, formal analysis, writing – original draft. Xiaohui Han: data curation, formal analysis. Shumin Li: formal analysis, investigation. Xuerui Zhang: formal analysis, writing – review & editing. Xiaodong Bi: supervision, conceptualization, validation, writing – review & editing, funding acquisition.

Conflicts of interest

There are no conflicts to declare.

Acknowledgements

This work is sponsored by National Natural Science Foundation of China (No. 22376126), Academic Promotion Program of Shandong First Medical University (No. 2019LJ003), and Shandong First Medical University Key Talent Introduction Project (No. 003083).

References

1 B. He, C. Lu, M. L. Wang, G. Zheng, G. Chen, M. Jiang, X. J. He, Z. X. Bian, G. Zhang and A. P. Lu, Drug Discovery in Traditional Chinese Medicine: From Herbal *fufang* to Combinatory Drugs, *Science*, 2015, **350**(6262), S74–S76.
2 C. Jiménez, Marine Natural Products in Medicinal Chemistry, *ACS Med. Chem. Lett.*, 2018, **9**(10), 959–961.
3 Y. F. Teng, L. Xu, M. Y. Wei, C. Y. Wang, Y. C. Gu and C. L. Shao, Recent Progresses in Marine Microbial-Derived Antiviral Natural Products, *Arch. Pharmacal Res.*, 2020, **43**(12), 1215–1229.
4 F. Chemat, M. Abert-Vian, A. S. Fabiano-Tixier, J. Strube, L. Uhlenbrock, V. Gunjevic and G. Cravotto, Green Extraction of Natural Products. Origins, Current Status, and Future Challenges, *TrAC, Trends Anal. Chem.*, 2019, **118**, 248–263.
5 S. Guo, S. Wang, J. Meng, D. Y. Gu and Y. Yang, Immobilized Enzyme for Screening and Identification of Anti-Diabetic Components from Natural Products by Ligand Fishing, *Crit. Rev. Biotechnol.*, 2023, **43**(2), 242–257.
6 X. F. Hou, M. Sun, T. Bao, X. Y. Xie, F. Wei and S. C. Wang, Recent Advances in Screening Active Components from Natural Products Based on Bioaffinity Techniques, *Acta Pharm. Sin. B*, 2020, **10**(10), 1800–1813.
7 R. P. Lively and D. S. Sholl, From Water to Organics in Membrane Separations, *Nat. Mater.*, 2017, **16**(3), 276–279.
8 J. Chen, M. Wei and M. Meng, Advanced Development of Molecularly Imprinted Membranes for Selective Separation, *Molecules*, 2023, **28**(15), 5764.
9 H.-B. Liu, B. Li, L.-W. Guo, L.-M. Pan, H.-X. Zhu, Z.-S. Tang, W.-H. Xing, Y.-Y. Cai, J.-A. Duan, M. Wang, S.-N. Xu and X.-B. Tao, Current and Future Use of Membrane Technology in the Traditional Chinese Medicine Industry, *Sep. Purif. Rev.*, 2022, **51**(4), 484–502.
10 R. Kaliszan, P. Wiczling, M. J. Markuszewski and M. A. Al-Haj, Thermodynamic vs. extrathermodynamic modeling of chromatographic retention, *J. Chromatogr. A*, 2011, **1218**(31), 5120–5130.

11 K. Miyabe, Y. Matsumoto and G. Guiochon, Peak Parking-Moment Analysis. A Strategy for the Study of the Mass-Transfer Kinetics in the Stationary Phase, *Anal. Chem.*, 2007, **79**(5), 1970–1982.
12 X. Subirats, M. H. Abraham and M. Rosés, Characterization of Hydrophilic Interaction Liquid Chromatography Retention by a Linear Free Energy Relationship. Comparison To Reversed- and Normal-Phase Retentions, *Anal. Chim. Acta*, 2019, **1092**, 132–143.
13 Q. Li, G. W. Yin, J. Wang, L. K. Li, Q. Liang, X. Zhao, Y. Y. Chen, X. H. Zheng and X. F. Zhao, An Emerging Paradigm to Develop Analytical Methods Based on Immobilized Transmembrane Proteins and its Applications in Drug Discovery, *TrAC, Trends Anal. Chem.*, 2022, **157**, 12.
14 R. Tian, J. T. Yin, Q. Q. Yao, T. T. Wang, J. H. Chen, Q. Liang, Q. Li and X. F. Zhao, Development of an Allostery Responsive Chromatographic Method for Screening Potential Allosteric Modulator of Beta2-adrenoceptor from a Natural Product-Derived DNA-Encoded Chemical Library, *Anal. Chem.*, 2022, **94**(25), 9048–9057.
15 Y. Xue, Z. L. Zhang, G. Wang, S. R. Wan, Q. Li and X. F. Zhao, Protein Superglue Inspiredin *in situ* One-Step Site-Specific Immobilization of Beta2-Adrenoceptor and its Application in Bioactive Compound Screening from Cortex Magnoliae Officinalis, *J. Chromatogr. A*, 2023, **1690**, 12.
16 X. Ding, Y. Cao, Y. Yuan, Z. Gong, Y. Liu, L. Zhao, L. Lv, G. Zhang, D. Wang, D. Jia, Z. Zhu, Z. Hong, X. Chen and Y. Chai, Development of APTES-Decorated HepG2 Cancer Stem Cell Membrane Chromatography for Screening Active Components from Salvia miltiorrhiza, *Anal. Chem.*, 2016, **88**(24), 12081–12089.
17 J. Fu, Q. Jia, P. Liang, S. Wang, H. Zhou, L. Zhang, H. Wang, C. Gao, Y. Lv, S. Han and L. He, Enhanced Stability Designs of Cell Membrane Chromatography for Screening Drug Leads, *J. Sep. Sci.*, 2022, **45**(14), 2498–2507.
18 W. Ma, C. Wang, R. Liu, N. Wang, Y. Lv, B. Dai and L. He, Advances in Cell Membrane Chromatography, *J. Chromatogr. A*, 2021, **1639**, 461916.
19 M. Mock, S. Edavettal, C. Langmead and A. Russell, AI Can Help to Speed Up Drug Discovery - But Only If We Give It the Right Data, *Nature*, 2023, **621**(7979), 467–470.
20 V. J. Sahayasheela, M. B. Lankadasari, V. M. Dan, S. G. Dastager, G. N. Pandian and H. Sugiyama, Artificial Intelligence in Microbial Natural Product Drug Discovery: Current and Emerging Role, *Nat. Prod. Rep.*, 2022, **39**(12), 2215–2230.
21 N. Savage, Drug Discovery Companies are Customizing Chatgpt: Here's How, *Nat. Biotechnol.*, 2023, **41**(5), 585–586.
22 F. L. Wong, C. de la Fuente-nunez and J. J. Collins, Leveraging Artificial Intelligence in The Fight against Infectious Diseases, *Science*, 2023, **381**(6654), 164–170.
23 B. Narasimhan, D. Sharma and P. Kumar, Biological Importance of Imidazole Nucleus in the New Millennium, *Med. Chem. Res.*, 2011, **20**(8), 1119–1140.
24 D. A. Shitov, D. V. Krutin and E. Y. Tupikina, Mutual Influence of Non-Covalent Interactions Formed by Imidazole: A Systematic Quantum-Chemical Study, *J. Comput. Chem.*, 2024, 15.
25 N. Rani, P. Kumar, R. Singh, D. P. de Sousa and P. Sharma, Current and Future Prospective of a Versatile Moiety: Imidazole, *Curr. Drug Targets*, 2020, **21**(11), 1130–1155.
26 H. V. Tolomeu and C. A. M. Fraga, Imidazole: Synthesis, Functionalization and Physicochemical Properties of a Privileged Structure in Medicinal Chemistry, *Molecules*, 2023, **28**(2), 27.
27 X. W. Zhu, D. Luo, X. P. Zhou and D. Li, Imidazole-based Metal-Organic Cages: Synthesis, Structures, and Functions, *Coord. Chem. Rev.*, 2022, **454**, 37.
28 J. Guo, Q. L. Yang, Q. W. Meng, C. H. Lau and Q. C. Ge, Membrane Surface Functionalization with Imidazole Derivatives to Benefit Dye Removal and Fouling Resistance in Forward Osmosis, *ACS Appl. Mater. Interfaces*, 2021, **13**(5), 6710–6719.
29 X. P. Song, C. Wang, S. S. Li, H. P. Liu and C. H. Zhang, Polyamide-Poly (Ionic Liquid) Reverse Osmosis Membrane with Manifold Excellent Performance Prepared via Bionic Capillary Network for Seawater Desalinization, *J. Membr. Sci.*, 2021, **632**, 9.
30 C. S. Lee, N. U. Kim, J. T. Park and J. H. Kim, Imidazole-Functionalized Hydrophilic Rubbery Comb Copolymers: Microphase-Separation and Good Gas Separation Properties, *Sep. Purif. Technol.*, 2020, **242**, 9.
31 S. Zeng, Y. H. Wang, Y. M. Zhou, W. L. Li, W. B. Zhou, X. Zhou, M. Wang, X. Q. Zhao and L. Ren, Mixed-Linker Synthesis of L-Histidine@Zeolitic Imidazole Framework-8 on Amyloid Nanofibrils-Modified Polyacrylonitrile Membrane with High Separation and Antifouling Properties, *Sep. Purif. Technol.*, 2022, **290**, 10.
32 X. Bi, M. Xie, C. Zhang, J.-M. Lin and R.-S. Zhao, Composite SPE Paper Membrane Based on the Functional Superstructure of Metal-Organic Frameworks and Ionic Liquids for Detection of Tetracycline-like Antibiotics, *ACS Appl. Mater. Interfaces*, 2022, **14**(1), 2102–2112.
33 S. Dutta, W. Mandal, A. V. Desai, S. Fajal, G. K. Dam, S. Mukherjee and S. K. Ghosh, A Luminescent Cationic MOF and its Polymer Composite Membrane Elicit Selective Sensing of Antibiotics and Pesticides in Water, *Mol. Syst. Des. Eng.*, 2023, 9.
34 G. Chen, X. Zeng and J. H. Huang, Imidazole-Modified Polymers and Their Adsorption of Salicylic Acid from Aqueous Solution, *J. Polym. Res.*, 2022, **29**(7), 7.
35 D. Depuydt, A. Van den Bossche, W. Dehaen and K. Binnemans, Metal Extraction with A Short-Chain Imidazolium Nitrate Ionic Liquid, *Chem. Commun.*, 2017, **53**(38), 5271–5274.
36 Z. K. Gu, Z. C. Guo, S. Gao, L. R. Huang and Z. Liu, Hierarchically Structured Molecularly Imprinted Nanotransducers for Truncated HER2-Targeted Photodynamic Therapy of Therapeutic Antibody-Resistant Breast Cancer, *ACS Nano*, 2023, **17**(11), 10152–10163.
37 S. X. Xu, Z. K. Gu, H. F. Lu, P. X. Guan and Z. Liu, Leveraging Macrophage-Mediated Cancer Immunotherapy via a Cascading Effect Induced by a Molecularly Imprinted

Nanocoordinator, *ACS Appl. Mater. Interfaces*, 2023, **15**(23), 27658–27669.

38 M. H. Zhao, P. X. Guan, S. X. Xu, H. F. Lu and Z. Liu, Molecularly Imprinted Nanomedicine for Anti-angiogenic Cancer Therapy via Blocking Vascular Endothelial Growth Factor Signaling, *Nano Lett.*, 2023, **23**(18), 8674–8682.

39 G. F. Li, Y. P. Wang, Y. H. Ding, Z. X. Zhang, N. Tang, X. P. Tian and D. J. Li, Fluorescent Nanosensors for Selective and Sensitive Determination of Isoquercitrin Based on Boronate Affinity-Based Imprinted Quantum Dots, *New J. Chem.*, 2023, **47**(18), 8942–8950.

40 R. R. Xing, T. Y. Xue, P. Ye, L. Yang, R. Q. Wang, X. Chen and S. Hu, pH-Responsive Epitope-Imprinted Magnetic Nanoparticles for Selective Separation and Extraction of Chlorogenic Acid and Caffeic Acid in Traditional Chinese Medicines, *Anal. Methods*, 2022, **14**(47), 4931–4937.

41 X. Zhang, L. Gao, L. Niu and X. Bi, Microwave-Assisted Preparation of a Molecularly Imprinted Monolith Combining an Imidazolium Ionic Liquid and POSS for Enhanced Extraction of Baicalin-Like Compounds in *Scutellaria Baicalensis* by Means of In-Capillary SPME Followed by On-Line LC and Off-Line LC-MS/MS, *New J. Chem.*, 2021, **45**(11), 5195–5205.

42 G. I. Salentijn, M. Grajewski and E. Verpoorte, Reinventing (Bio)chemical Analysis with Paper, *Anal. Chem.*, 2018, **90**(23), 13815–13825.

43 B. Singh, J. P. Singh, A. Kaur and N. Singh, Antimicrobial Potential of Pomegranate Peel: A Review, *Int. J. Food Sci. Technol.*, 2019, **54**(4), 959–965.

44 Chinese Pharmacopoeia Commission, *The State Pharmacopoeia Commission of People's Republic of China*, Chemical Industry Press, Beijing, China, 2020, vol. 1.

45 A. R. Fontana and R. Bottini, High-Throughput Method Based on Quick, Easy, Cheap, Effective, Rugged and Safe Followed by Liquid Chromatography-Multi-Wavelength Detection for the Quantification of Multiclass Polyphenols in Wines, *J. Chromatogr. A*, 2014, **1342**, 44–53.

46 M. Ghani, R. M. Frizzarin, F. Maya and V. Cerdà, In-Syringe Extraction Using Dissolvable Layered Double Hydroxide-Polymer Sponges Templated from Hierarchically Porous Coordination Polymers, *J. Chromatogr. A*, 2016, **1453**, 1–9.

47 G. Karasová, J. Lehotay, J. Sádecká, I. Skacáni and M. Lachová, Selective Extraction Of Derivates of *p*-Hydroxy-Benzoic Acid From Plant Material by Using a Molecularly Imprinted Polymer, *J. Sep. Sci.*, 2005, **28**(18), 2468–2476.

48 F. F. Chen, G. Y. Wang and Y. P. Shi, Molecularly Imprinted Polymer Microspheres for Solid-Phase Extraction of Protocatechuic Acid in *Rhizoma Homalomenae*, *J. Sep. Sci.*, 2011, **34**(19), 2602–2610.

49 Y. Hao, R. X. Gao, D. C. Liu, Y. H. Tang and Z. J. Guo, Selective Extraction of Gallic Acid in *Pomegranate Rind* Using Surface Imprinting Polymers over Magnetic Carbon Nanotubes, *Anal. Bioanal. Chem.*, 2015, **407**(25), 7681–7690.

50 C. Wang, X. J. Li, J. Yang, Y. X. Zhao, Z. S. Liu and H. A. Aisa, Preparation of Ionic Liquid-Mediated Imprinted Monolith for Selective Capture and Purification of Corilagin, *J. Chromatogr. B*, 2017, **1041**, 98–103.

51 J. J. Zhang, B. Q. Li, H. J. Yue, J. Wang and Y. S. Zheng, Highly Selective and Efficient Imprinted Polymers Based on Carboxyl-Functionalized Magnetic Nanoparticles for the Extraction of Gallic Acid From *Pomegranate Rind*, *J. Sep. Sci.*, 2018, **41**(2), 540–547.

52 X. Bi, L.-X. Zhao, M. Xie, C. Zhang, J.-M. Lin and R.-S. Zhao, Functional Metal-Organic Framework as High-Performance Adsorbent for Selective Enrichment of Pharmaceutical Contaminants in Aqueous Samples, *Chem. Eng. J.*, 2022, **445**, 136751.

53 M. C. Hutter, Differential Multimolecule Fingerprint for Similarity Search-Making Use of Active and Inactive Compound Sets in Virtual Screening, *J. Chem. Inf. Model.*, 2022, **62**(11), 2726–2736.

54 A. Daina, O. Michielin and V. Zoete, Swiss Target Prediction: Updated Data And New Features for Efficient Prediction of Protein Targets of Small Molecules, *Nucleic Acids Res.*, 2019, **47**(W1), W357–W364.

55 H. Y. Li, L. Zhang, W. J. Yu, W. W. Bie, M. J. Wei, Z. X. Wang, F. Y. Kong and W. Wang, Sulfonated Polyhedral Oligomeric Silsesquioxane-Cyclodextrin Hybrid Polymers for Efficient Removal of Micropollutants from Water, *Carbohydr. Polym.*, 2023, **312**, 11.

56 X. Q. Qiao, R. Chen, H. Y. Yan and S. G. Shen, Polyhedral Oligomeric Silsesquioxane-Based Hybrid Monolithic Columns: Recent Advances in Their Preparation and Their Applications in Capillary Liquid Chromatography, *TrAC, Trends Anal. Chem.*, 2017, **97**, 50–64.

57 Japanese National Institute of Advanced Industrial Science and Technology (AIST), *Spectral Database for Organic Compounds*, 2022, **https://sdbs.db.aist.go.jp/sdbs/cgi-bin/cre_index.cgi?lang=eng#opennewwindow**.

58 S. Goutelle, M. Maurin, F. Rougier, X. Barbaut, L. Bourguignon, M. Ducher and P. Maire, The Hill Equation: A Review of Its Capabilities in Pharmacological Modelling, *Fundam. Clin. Pharmacol.*, 2008, **22**(6), 633–648.

59 L. Ye, B. Zhong, M. Huang, W. Chen and X. Wang, Pollution Evaluation and Children's Multimedia Exposure of Atmospheric Arsenic Deposition in The Pearl River Delta, China, *Sci. Total Environ.*, 2021, **787**, 147629.

60 P. F. Li, S. Gao, W. T. Qu, Y. Li and Z. Liu, Chemo-Selective Single-Cell Metabolomics Reveals the Spatiotemporal Behavior of Exogenous Pollutants During Xenopus Laevis Embryogenesis, *Adv. Sci.*, 2023, 12.

61 X. Bi, X.-L. Wang, L.-X. Zhao, M. Xie, X.-W. Zhao, C. Zhang, R.-S. Zhao and B. Guo, Enrichment of Antivirally-Active Compounds Using Metal-Organic Frameworks Tailored with Quecher-Oriented Solvent Adaptability and Selectivity, *Microchem. J.*, 2024, **198**, 110188.